INTERNATIONAL JOURNAL OF CLIMATOLOGY
Int. J. Climatol. **28**: 1761–1774 (2008)
Published online 28 January 2008 in Wiley InterScience
(www.interscience.wiley.com) DOI: 10.1002/joc.1590

The global footprint of persistent extra-tropical drought in the instrumental era

Celine Herweijer[1]* and Richard Seager[2]
[1] *Risk Management Solutions, London, UK*
[2] *Lamont Doherty Earth Observatory, Columbia University, USA*

ABSTRACT: The major North American droughts as per instrumental records are shown to be part of a larger, global pattern of low-frequency drought variability. Drought in western North America during the 1850s–1860s, 1870s, 1890s, 1930s and 1950s, is shown to coincide with the occurrence of prolonged dry spells in parts of Europe, southern South America and western Australia. Tropical land regions are mostly wet during these periods, with the exception of central east Africa, southern India and Sri Lanka, which are dry. The recent 1998–2003 period of drought in western North America reveals a similar global hydroclimatic 'footprint' with the exception of a wet southern South America and continued dry conditions in the Sahel. Common to each of the six droughts is the persistence of anomalously cool east central tropical Pacific sea surface temperatures (SSTs). For the 1998–2003 case, the warming of SSTs everywhere outside of the east central tropical Pacific may be influencing precipitation and masking the influence of persistent precipitation anomalies driven from the tropical Pacific alone. In general, examination of these major historical extra-tropical droughts reveals a hemispherically and, in the extra-tropics, a zonally symmetric pattern consistent with forcing from the Tropics.

Ensembles of model simulations forced by observed SSTs globally (Global Ocean Global Atmosphere, GOGA) and only within the tropical Pacific (Pacific Ocean Global Atmosphere-Mixed Layer, POGA-ML) are both able to capture the global pattern of the persistent extra-tropical drought regimes since the mid-nineteenth century. This implies that the recently demonstrated link between SST forcing and drought in North America is in fact only one part of a global hydroclimatic response to the persistence of cool SST anomalies in the tropical Pacific. Indian Ocean SST forcing is required to capture the droughts in central east Africa. Over Europe, the modelled, low-frequency precipitation signal is unrealistically ENSO dominated, as the model does not faithfully reproduce the observed history of low-frequency NAO variability. Overall, our results suggest that the global pattern of persistent drought appears to be a low-frequency version of interannual ENSO-forced variability.

Received 20 December 2005; Revised 30 May 2007; Accepted 3 June 2007

1. Introduction

Multi-year droughts are a devastating, complex and staggeringly expensive natural hazard. In North America, the most severe multi-year droughts of the last 150 years were the 'Civil War' drought (1856–1865), the 1870s and 1890s droughts, the infamous Dust Bowl drought of the 1930s, the late 1940s–mid 1950s southwestern drought and the present-day drought that has gripped the West since 1998 (Woodhouse and Overpeck, 1998; Cole *et al*., 2002; Fye *et al*., 2003; Herweijer *et al*., 2006; Seager *et al*., 2005a). In the southern part of South America, in a semi-arid area that encompasses the Andean foothills, the Sierra Cordoba and the Pampas in Argentina, along with Uruguay and southern Brazil, extended dry spells have also been noted in the 1930s and 1950s (Mechoso and Iribarren, 1992; Scian and Donnari, 1997; Robertson and Mechoso, 1998; Compagnucci *et al*., 2002), and inferred from tree-ring data in the 1860s and 1870s (Villalba *et al*., 1998). In addition, widespread drought conditions have been documented over much of central and eastern northern Europe during the 1860s (Hulme and Jones, 1994), 1890s, 1930s and the late 1940s/early 1950s (Briffa *et al*., 1994) and over the European part of the Former Soviet Union (FSU) during the 1890s and 1930s (Meshcherskaya and Blazhevich, 1997). Hoerling and Kumar (2003) noted that the most recent drought (which began in 1998) stretched from North America to Asia, but the in-phase relationship of global historical droughts with North American drought has, until now, been overlooked.

Much recent attention has been focussed on understanding the nature, extent and forcing of drought in the western United States (Hoerling and Kumar, 2003; Fye *et al*., 2004; Schubert *et al*., 2004a; Herweijer *et al*., 2005; Seager *et al*., 2005a). Cole *et al*. (2002) and Fye *et al*. (2004) noted that persistently cold tropical Pacific sea surface temperature (SST) anomalies have co-occurred with the major North American droughts since the mid-nineteenth century. It is well known that on interannual timescales, La Niña winters are characterized by reduced precipitation over much of the northern subtropics and mid-latitudes, particularly over western North

* Correspondence to: Celine Herweijer, 30 Monument Street, London EC3R 8NB, UK. E-mail: celineherweijer@rms.com

America (Trenberth and Branstator, 1992; Trenberth and Guillemot, 1996; Cole *et al*., 2002; Seager *et al*., 2005b). Recently, it has also been demonstrated that over longer timescales, a persistently cool tropical Pacific can provide the steady atmospheric forcing necessary for North American drought: each persistent North American drought since the 1850s has been simulated in an ensemble of climate model simulations forced by the observed history of tropical Pacific SSTs alone (Seager *et al*., 2005a; Herweijer *et al*., 2005; Huang *et al*., 2005). In the extratropics, alongside zonal asymmetries produced by Rossby wave propagation from the cooler equatorial Pacific, a zonally and hemispherically symmetric component to the forcing is observed. This pattern is a lower frequency realization of the subtropical jet – transient eddy – mean meridional circulation interaction mechanism (the Tropical Modulation of Mid-latitude Eddies, TMME, mechanism) that works throughout the year to promote eddy-driven descent in mid-latitudes when the tropical Pacific is cool (Seager *et al*., 2003, 2005a,b; Robinson, 2005). The existence of this mechanism suggests that drought over North America should appear as part of a larger, global pattern of mid-latitude drought. However, whether such a global pattern of persistent extra-tropical drought occurs in nature has thus far not been demonstrated.

Here we extend this recent work, which was largely focussed on North American drought, and examine the *global* hydroclimatic context of the major extra-tropical drought regimes (Here we us the dictionary definition of *regime*: 'the characteristic behaviour or orderly procedure of a natural phenomenon or process' (Webster's Ninth New Collegiate Dictionary) and do not mean to imply a non-linear process) of the past 150 years. Using historical precipitation data, and proxy data for the earliest drought, we make the case that each of the famous North American dry events can be considered as part of a global, hemispherically symmetric hydroclimatic regime. To demonstrate the extent to which these hemispherically symmetric droughts are tropically forced, and to identify regions in which SSTs from outside the tropical Pacific play an important role, the two ensembles of simulations with an atmosphere general circulation model (AGCM) that have been previously analysed by the authors are further examined. The first ensemble forces an atmospheric model with observed SSTs everywhere; the second forces the atmosphere model only with tropical Pacific SSTs. We will show that the models simulate each of the major multi-year extra-tropical drought regimes since the mid-nineteenth century, including the observed coincident dryness in much of Europe and central Asia and western North America in the northern hemisphere, and southern South America in the southern hemisphere. The hydroclimate regime throughout the global tropics includes wet conditions in the Sahel, and drought in central east Africa, features that are also captured by the models. Meanwhile, the coincident droughts in western Australia are less well captured by the models. Furthermore, we will demonstrate that this global hydroclimatic pattern is largely reproduced when the forcing is limited to the tropical Pacific region. We will also show that the spatial pattern of extreme and persistent drought is a low-frequency component of the large-scale climate variability associated with the El Niño southern oscillation (ENSO).

2. Synchronous large-scale extra-tropical droughts

2.1. Observed history

The global context of six well-known periods of severe and prolonged drought in North America is examined: the droughts of the 1850s–1860s, 1870s, 1890s, 1930s and 1950s (Fye *et al*., 2004) and the recent drought from 1998 to 2003 (The period since 1998 marks the most recent occurrence of multi-year drought in North America. Drought conditions returned to the Northern Rocky Mountains and the Pacific northwest as of Autumn 2005, but were interrupted in the central mid-west and the Pacific coast in early 2004 and late 2004 respectively. As such, we focus here on the 1998–2003 period of widespread drought in western North America).

2.1.1. SSTs

The average observed SST anomaly for each interval of persistent drought is shown in Figure 1. The SST data (Kaplan *et al*., 1998; Rayner *et al*., 2003) is that used to force the model experiments outlined in Section 2.2 (for details see Herweijer *et al*., 2005; Seager *et al*., 2005a). Each of the dry episodes coincides with the persistence of anomalously cool tropical Pacific SSTs. A cool Indian Ocean, typical of La Niña conditions, accompanies each drought with the notable exception of the most recent event. For the 1998–2003 period, SSTs everywhere outside of the tropical Pacific are anomalously warm, consistent with the global warming trend relative to the 1856–2004 mean. During the 1930s and 1950s droughts, while the tropical Pacific was cool, the north Atlantic Ocean was warm. Such a warm north Atlantic has been suggested to be important for simulating the Dust Bowl drought in several recent model studies (Schubert *et al*., 2004b; Sutton and Hodson, 2005). While that is possible, it is noteworthy that during the three nineteenth century droughts, the north Atlantic was not notably warmer than the Pacific.

2.1.2. Station precipitation data

Averages of the global precipitation anomaly from the Global Historical Climate Network (GHCN) data-set (described by Eischeid *et al*., 1991) for each of these drought events are shown in Figure 2. The station data is binned into boxes of four degrees of latitude and longitude and must be interpreted with caution in the mid-nineteenth century as data is scarce outside of Europe. The recent drought aside, persistent drought in North America is consistently accompanied by extra-tropical drought in the South American region encompassing north and central Argentina, Uruguay and

DOI: 10.1002/joc

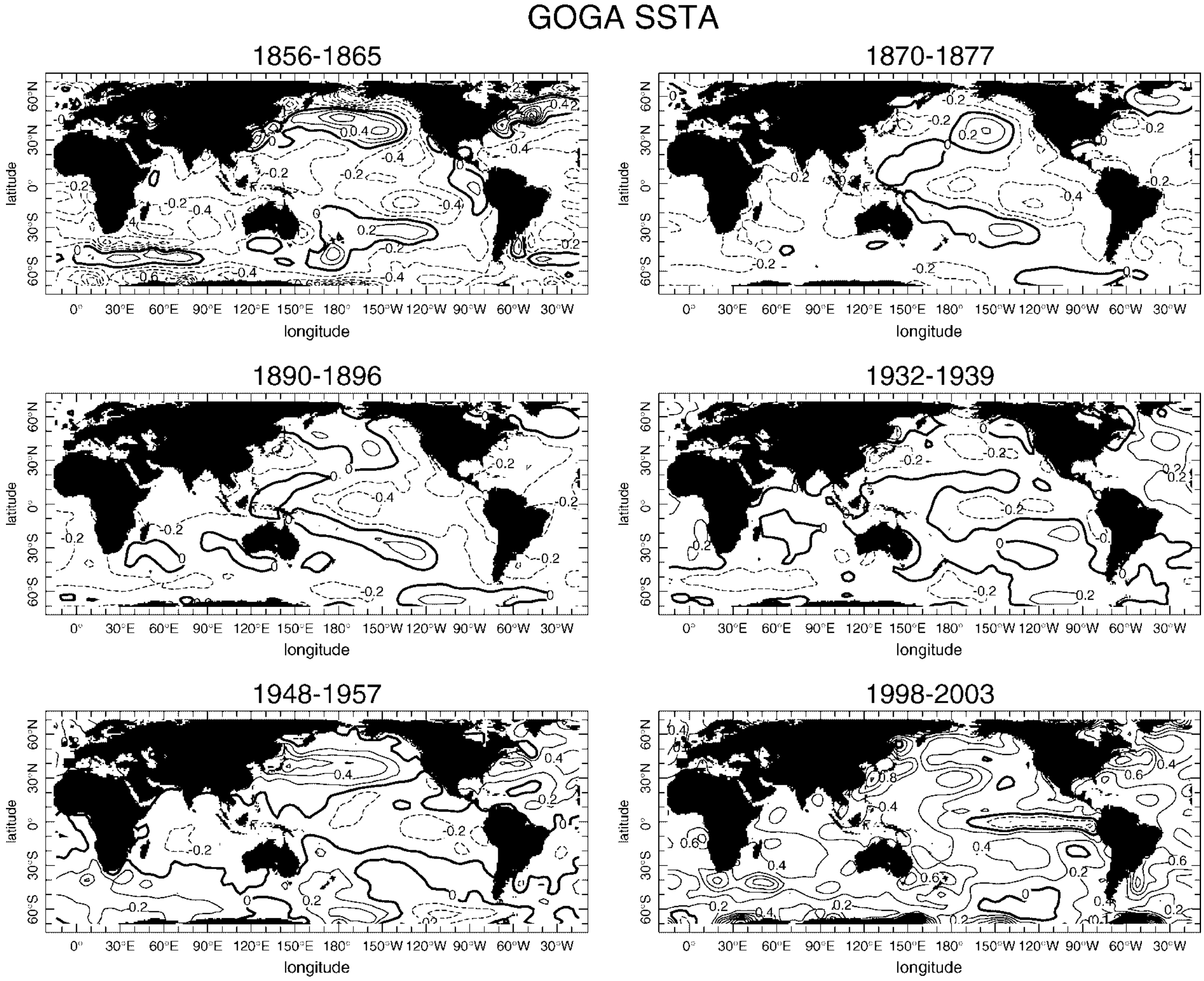

Figure 1. Observed SST anomalies during selected major North American drought regimes of the instrumental period. Temperature units are K. The SST field is that used in the GOGA ensemble mean. (N.B. The POGA-ML model is only forced by tropical Pacific SSTs between 20 °N and 20 °S). All anomalies are relative to the 1856–2004 mean.

southern Brazil. The in-phase relationship between low-frequency drought/wetness in the Americas is further highlighted by the high correlation ($r = 0.57$ at $p < 0.01$) between the 6-year low-pass filtered precipitation anomalies averaged over the southwestern United States (25 °N–35 °N; 95 °W–120 °W) and over Uruguay and the Pampas in Argentina (35 °S–45 °S; 50 °W–65 °W) since 1900 (Figure 3). The 6-year low-pass filter is applied to remove the effects of interannual variability, retaining variability on timescales of just under a decade and longer. The 1998–2003 period is an exception: southern South America was anomalously wet (Figure 2).

There is a clear tendency for drought to occur over large parts of Europe at the same time there is drought in North America (Figure 2). In the 1998–2003 case, dry conditions are restricted to southern and central Europe. The 1930s are a clear exception, with most of Europe recording wetter than normal conditions. Australia tends to be dry in the west during these times and wet in the east, with the 1930s again being an exception when the entire continent was dry and the most recent pattern being indistinct. Tropical land regions including central America, tropical South America, north Africa including the Sahel (except for the recent drought), southern Africa, the maritime continent and eastern Australia (except for the 1930s) are mostly wet during these persistent mid-latitude dry spells. In contrast, equatorial east Africa (Tanzania, Kenya and Somalia), and the region encompassing southernmost India and Sri Lanka, are consistently dry during mid-latitude droughts. Precipitation over northeast Brazil is greatly influenced by both tropical Atlantic SSTs and tropical Pacific SSTs (Hastenrath and Heller, 1977; Moura and Shukla, 1981) and does not fall easily into the global pattern.

Apart from southern South America, the obvious difference between the global footprint of the most recent drought and its nineteenth and twentieth century predecessors is the Sahel. Precipitation here does respond to ENSO (Giannini *et al*., 2003), and the persistent La Niñas of the 1930s and 1950s could be responsible for wet conditions during this time, but there has also been a multidecadal drying since the middle of the century, that has been related to warming of the tropical oceans (Giannini *et al*., 2003). Consequently, the Sahel has been dry during the most recent mid-latitude drought regime, unlike during prior regimes.

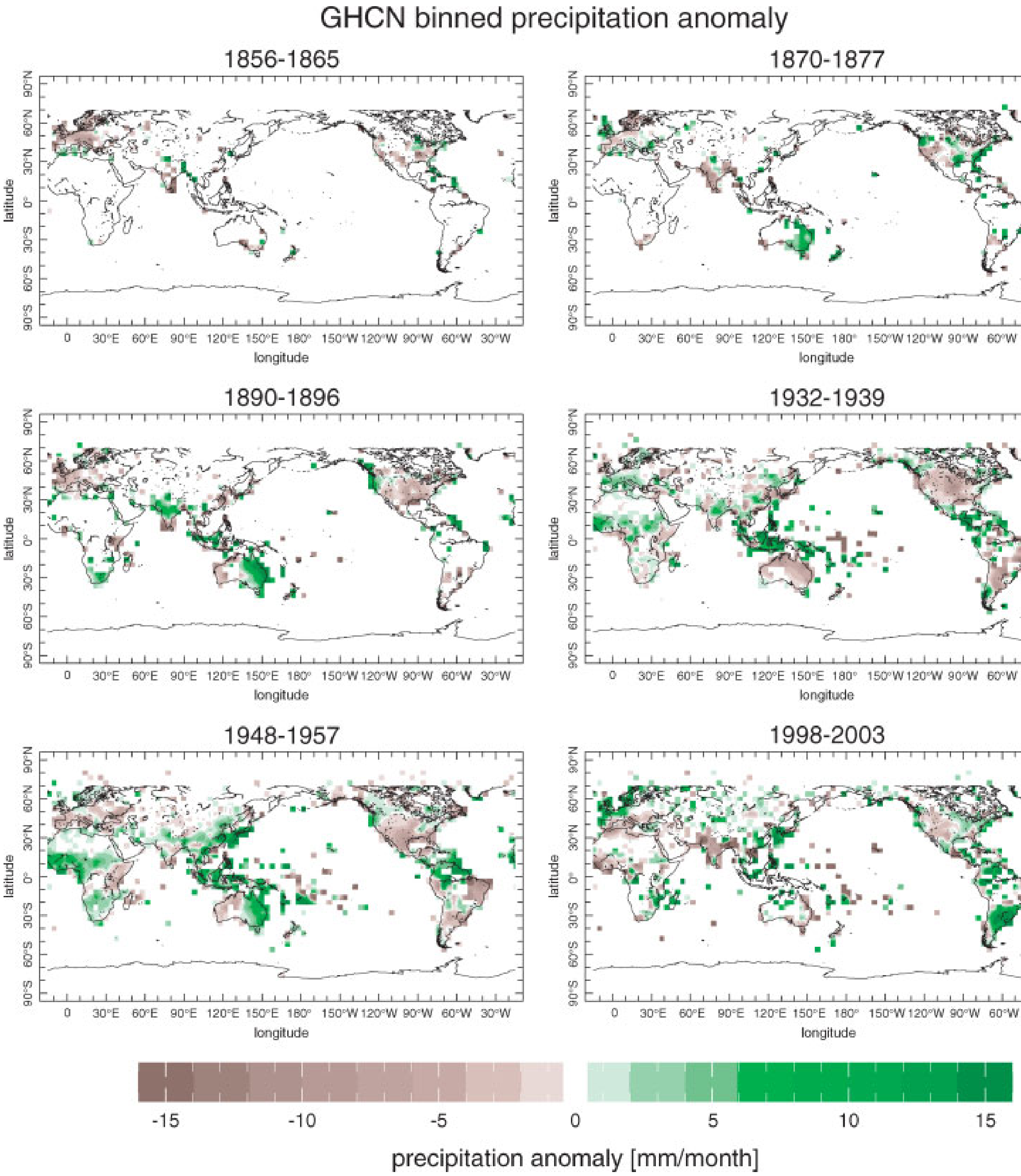

Figure 2. The observed Global Historical Climatological Network (GHCN) 4° × 4° gridded station data precipitation anomaly (mm/month) for selected major North American drought regimes of the instrumental period. All anomalies are relative to the 1856–2004 mean.

For the entire instrumental period, precipitation reductions during the persistent drought regimes amount to approximately 10% of the mean annual precipitation, with slightly greater deficits of up to 20% in the southwest United States. While these percentage reductions are small they are persistent and sufficient to cause hydrological drought.

2.1.3. *Historical and proxy data*

Beyond North America, Europe and parts of the Indian subcontinent, the GHCN instrumental record for the late- to mid-nineteenth century droughts becomes increasingly sparse. The global footprint of these drought regimes can be reconstructed further using historical references and proxy indicators. For the southern South America region, evidence from tree-ring data (Villalba *et al*., 1998) and stream flow data (Preito *et al*., 1999) point to drier than normal conditions in the late 1850s to early 1860s, the 1870s and the early 1890s. To the north, tree ring records from the Amazonian floodplains indicate wetter than normal conditions at these times (Schoengart *et al*., 2004), while Allan and D'Arrigo (1999), as an extension to the study by Quinn (1993), register a lack of El Niño related northeast Brazil droughts or 'Secas' in the 1860s (Quinn and Neal, 1992). Drought in Europe, though fairly well represented by the GHCN data, is further documented in the 1860s by Hulme and Jones (1994), by Casty *et al*. (2005) gridded precipitation reconstructions for the European Alps during the 1860s and 1890s, and by tree-ring reconstructions from the eastern Mediterranean during the late 1850s, the 1870s and the 1890s (Touchan *et al*., 2005). Each of the aforementioned reconstructions conforms to the global hydroclimatic pattern of the succeeding twentieth century drought regimes.

The proxy-derived hydroclimatic signature of the mid- to late-nineteenth century droughts on the African continent is more complicated. In North Africa, 1856–1865 is characterized by a mixed occurrence of low and high Nile River discharge levels (Riehl *et al*., 1979; Evans, 1990; Quinn, 1993), with the late 1850s marked by El Niño-related lowstands, which are absent in the early 1860s. The 1870s and early 1890s in the Nile records are more characteristic of a La Niña-like response, with both periods recording a consistent lack of El Niño-related lowstands (Quinn, 1993). Further south, historical accounts and lake level reconstructions from equatorial east Africa indicate lower water levels in the early- to mid-nineteenth century, followed by, in most cases, steadily rising levels in the following one to two decades (Sieger, 1887, 1888 (as referenced by Walsh and Musa, 1994); Owen and Crossley, 1989; Nicholson, 1998, 1999, 2001; Nicholson and Yin, 2001; Verschuren, 2001). However, the resolution and the complexity of interpreting these historical lake level records, hinders their interpretation on the multi-year timescales required here. In southern Africa, a region characteristically wet during most of the identified extra-tropical drought events, missionary documents from the Kalahari region (Endfield and Nash, 2002; Nash and Endfield, 2002), climate chronologies from the former Cape Province of South Africa (Lindesay and Vogel, 1990), and semi-quantitative southern African rainfall timeseries from Nicholson (2001) each indicate a dry late 1850s to early 1860s. Meanwhile, the 1870s and 1890s are both wet (Lindesay and Vogel, 1990; Nicholson, 2001), equivalent to a La Niña rainfall signal in this region. In summary, the historical and proxy evidence from northern and southern Africa display a mixed signal during the 1860s, whilst the 1870s and 1890s periods share the African hydroclimatic footprint of subsequent instrumental global drought regimes more convincingly.

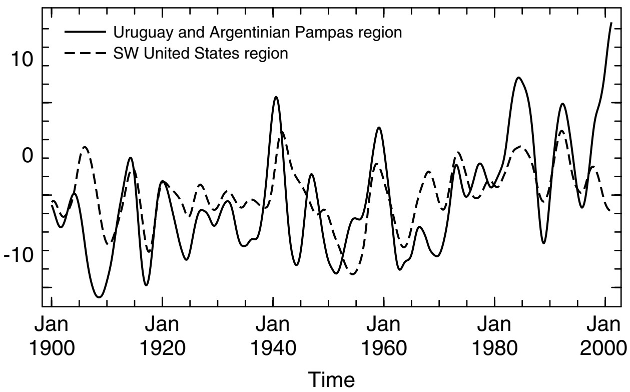

Figure 3. Timeseries of the 6-year low-pass filtered GHCN 4° × 4° gridded station data precipitation anomaly (mm/month) averaged over the southwest United States (25°–35°N; 95°–120°W), and Uruguay and the Pampas in Argentina (30°–40°S; 50°–65°W).

The hemispherically symmetric nature of these drought regimes implicates the notion of forcing from the tropics, a hypothesis that we now test.

2.2. Unravelling the role of SST forcing: a modelling approach

2.2.1. Climate model simulations

The set-up of the model experiments is akin to several previous studies that have examined the cause and nature of drought in North America (*cf* Herweijer *et al*., 2005; Seager *et al*., 2005a). Here we extend that work by examining the global precipitation response to SST forcing. Two climate model experiments are employed: the first forces an AGCM with the observed history of SSTs everywhere from 1856 to 2004 (the Global Ocean Global Atmosphere, (GOGA), model), the second forces the AGCM only with tropical Pacific SSTs (between 20 °N and 20 °S), being coupled to a two-layer entraining mixed layer (ML) ocean elsewhere (the Pacific Ocean Global Atmosphere, POGA-ML, model). A 16-member ensemble was performed for each experiment. The SST data is a combination of that of Kaplan *et al*. (1998) and the HadISST global dataset (Rayner *et al*., 2003). Further details of these simulations can be found in Seager *et al*. (2005a) [see also Herweijer *et al*., 2005 and Huang *et al*., 2005]. The AGCM used is the National Center for Atmospheric Research (NCAR) Climate Community Model 3 (CCM3) described in detail by Kiehl *et al*. (1998). We focus on the ensemble mean of each experiment-the part of the climate variability that is SST forced.

2.2.2. POGA-ML model-data comparison

Figure 4 shows averages of the modelled precipitation anomalies from the POGA-ML model for the selected major North American drought regimes, as shown in Figure 2. With forcing only from the tropical Pacific surface ocean, the model is able to simulate much of the observed pattern of mid-latitude drought. Each period of modelled North American drought is accompanied by drought over much of Europe extending into central Asia (a region with limited observational coverage before the 1960s), and, with the notable exception of the recent period, drought in the South American region of north and central Argentina, Uruguay and southern Brazil. For the 1998–2003 period, the POGA-ML model correctly makes southern South America wet, in contrast to creating droughts during the five previous instrumental drought regimes. However, the spread in the ensembles over this period (not shown) is too large to conclude that the wetness in this region is forced by tropical Pacific SSTs. The POGA-ML model does less well in capturing the observed western Australian droughts. Wetter than

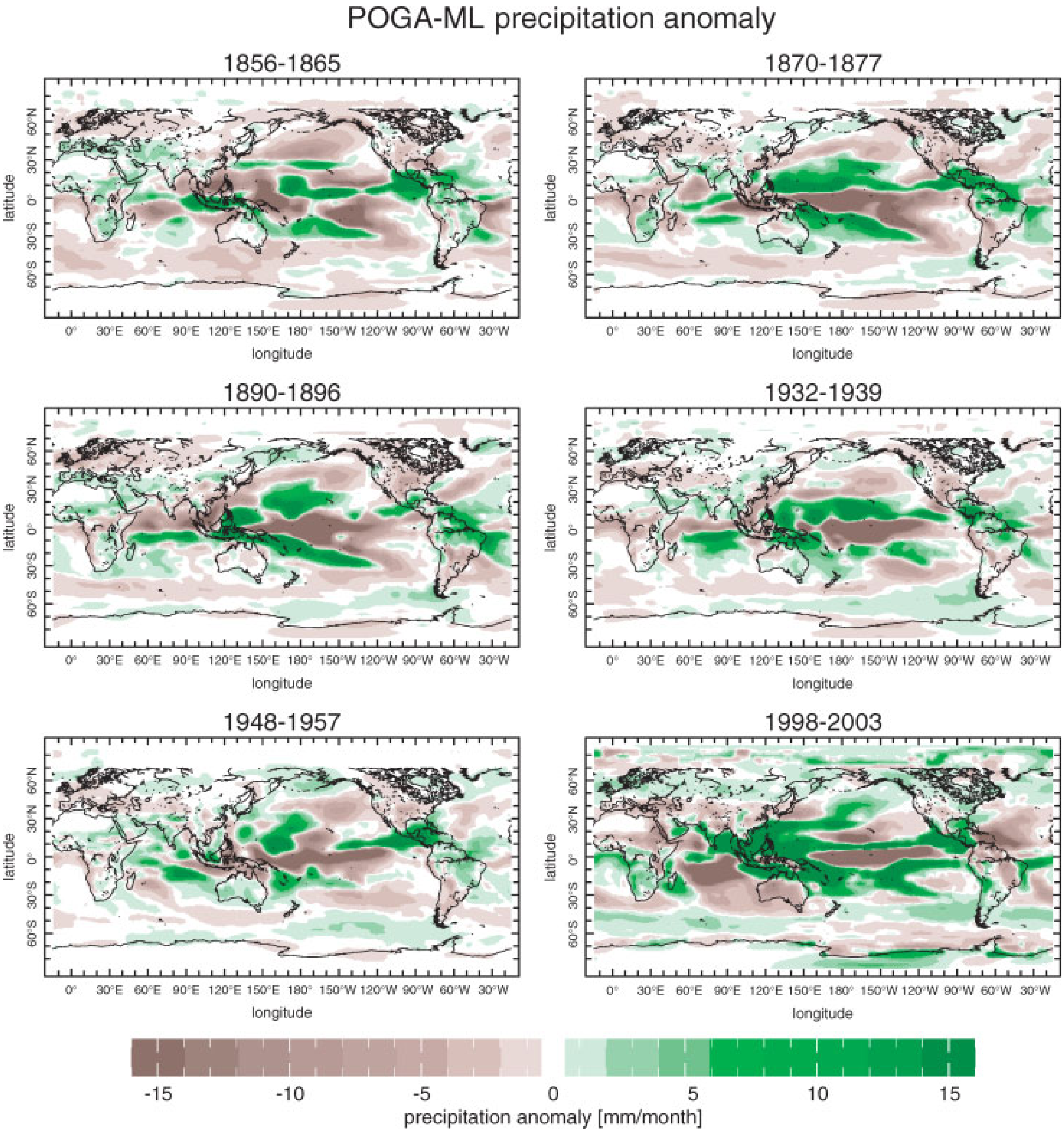

Figure 4. The POGA-ML modelled global precipitation anomaly (mm/month) for selected major North American drought regimes of the instrumental period. All anomalies are relative to the 1856–2004 mean.

normal conditions are simulated in central America, the Sahel (except for the recent period, as explained in Section 2.1), south Africa, and the southern Mediterranean, as observed.

2.2.3. GOGA model-data comparison

Including the forcing from the global ocean generally gives a comparable picture (Figure 5). It is noted that for the 1998–2003 period, wet anomalies are more frequent than dry anomalies in most places-representative of the rather clear global mean global warming signal. As for the POGA-ML experiment, the western Australian droughts are poorly simulated. SSTs from outside the tropical Pacific are required to capture the droughts in equatorial east Africa, consistent with prior work on the impact of Indian Ocean SSTs (Goddard and Graham, 1999). Here, cooler SSTs and diminished convective heating in the west central Indian Ocean leads to anomalous moisture flux divergence and reduced rainfall over equatorial east Africa. These findings are consistent with ours, in that the observed central east African droughts are only captured when forcing from a cool west central Indian ocean is included (i.e. in the GOGA model, Figure 5). During the 1930s the Indian Ocean SST anomalies are muted, as is the corresponding east central African drought in both the model and in the observations. Similarly, during the 1998–2003 period the Indian Ocean, like all surface waters outside of the cool eastern tropical Pacific, is anomalously warm and the model does not produce a drought while the observed record was itself indistinct.

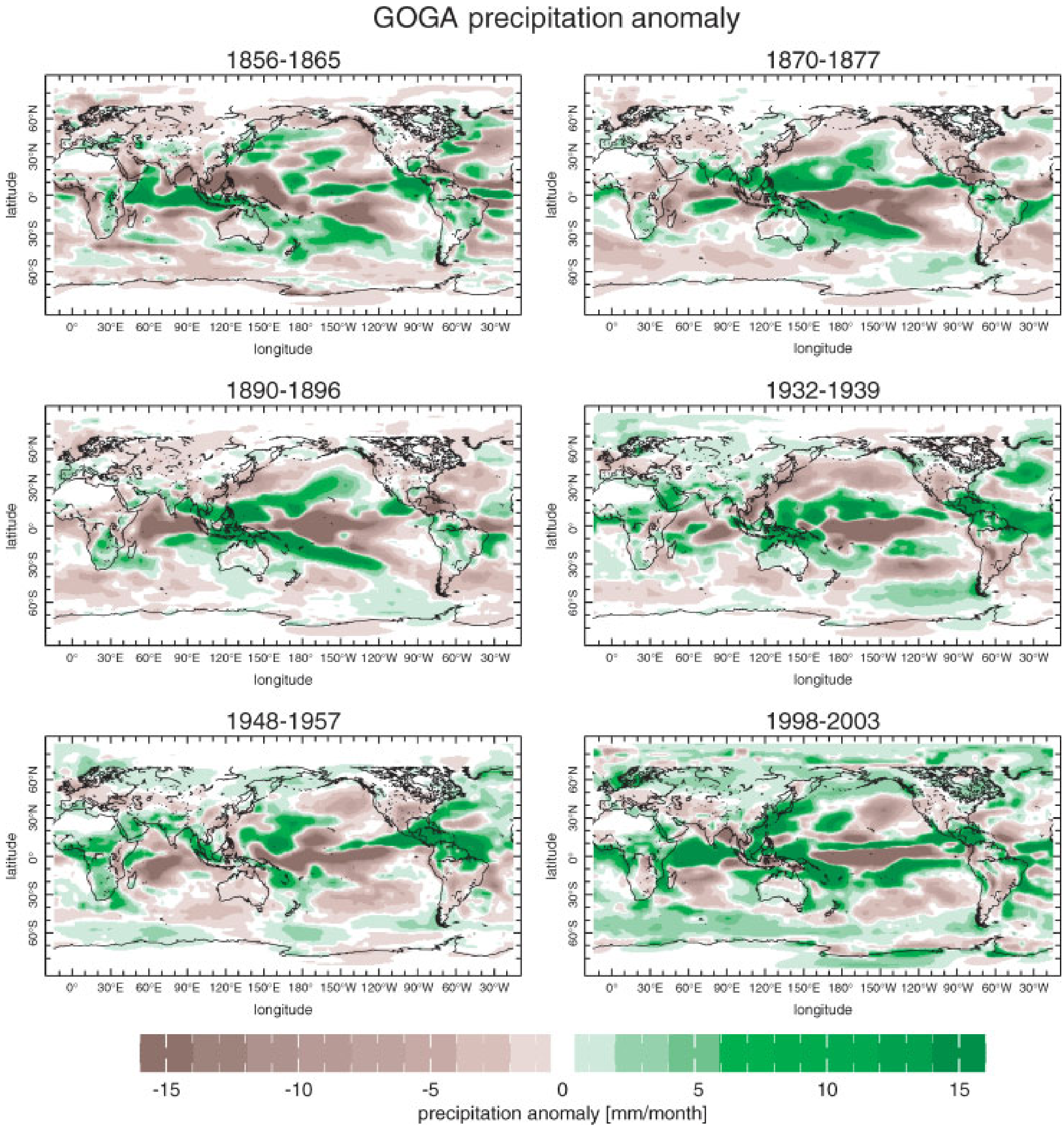

Figure 5. The GOGA modelled global precipitation anomaly (mm/month) for selected major North American drought regimes of the instrumental period. All anomalies are relative to the 1856–2004 mean.

A potential flaw of the GOGA experiment concerns the impact of specified SSTs on annular mode variability, and the associated component of extra-tropical precipitation variability (e.g. Hurrell, 1995; Hurrell *et al*., 2003). Annular modes are internal atmospheric modes that drive extra-tropical SST anomalies (e.g. Seager *et al*., 2000; Visbeck *et al*., 2003). A long-standing question has been the extent to which anomalous extra-tropical SSTs feed back to affect the atmosphere (e.g. Rodwell *et al*., 1999; Robinson, 2000; Kushnir *et al*., 2002). It has been shown that AGCMs forced with observed SST anomalies can reproduce the annular mode behaviour that induced these extra-tropical SST anomalies (Rodwell *et al*., 1999). However, almost by construction, the surface flux anomalies are the wrong sign-i.e. out of the ocean in a region where the annular mode makes the SST warm and the flux should in reality be into the ocean. As such, it is unclear whether the atmospheric response represents a real response to the SST anomalies, or whether it is an artifact of the misrepresentation of the atmosphere-ocean coupling in the model (Barsugli and Battisti, 1998; Bretherton and Battisti, 2000), with the potential to introduce errors in the precipitation signal. If, as argued by Hoerling *et al*. (2001), annular mode variability is forced from the tropical oceans, the AGCM experiments presented here may be able to simulate the observed changes. On the other hand, if annular mode variability is driven primarily by internal atmospheric variability, or if it responds to external factors such as changing atmospheric trace gas composition (Shindell

DOI: 10.1002/joc

et al., 1999) that we neglected in the model experiments, it is likely that there is a component of extra-tropical precipitation variability that the models will not capture.

The above factor is likely to be important over the European sector, where precipitation variability is strongly influenced by the North Atlantic oscillation (NAO) (Hurrell, 1995; Dai *et al*., 1997), and to a lesser extent by the remote tropical Pacific climate (Dai *et al*., 1997; Merkel and Latif, 2002; Seager *et al*., 2005b; Mariotti *et al*., 2005). A multivariate regression of the GHCN precipitation anomalies onto the 6-year low-pass filtered NAO index (Hurrell, 1995) and NINO3 index (Kaplan *et al*., 2003) highlights the relative impact of low-frequency NAO- and ENSO-related climate variability on this region (Figure 6). This is done for the months of December through March, from 1863 to 1995, corresponding to the NAO index of Hurrell (1996). The correlation between NAO variability and European precipitation is in general higher than for low-frequency ENSO variability (Figure 6(b) and (d)) which is decidedly weak.

Overall, approximately 20% of the low-frequency precipitation variability over Europe is explained by the combined influence of low-frequency ENSO- and NAO-related climate variability. During the mid- to late-1930s, (Hurrell, 1996) the winter NAO index was persistently negative, a factor that may explain the observed wet central and southern Europe at that time (Figure 2). The model does not faithfully reproduce the low-frequency variations of the NAO. As such, the European low-frequency precipitation in the model is ENSO-dominated and creates a spurious drought in the 1930s. Although the relationship between tropical Pacific SSTs and European rainfall is weak the model simulations quite consistently make parts of Europe dry during protracted La Niña-like states. In agreement, parts or nearly all of Europe were struck by drought in the 1850s, 1870s, 1890s and 1950s. The south European and Mediterranean drought

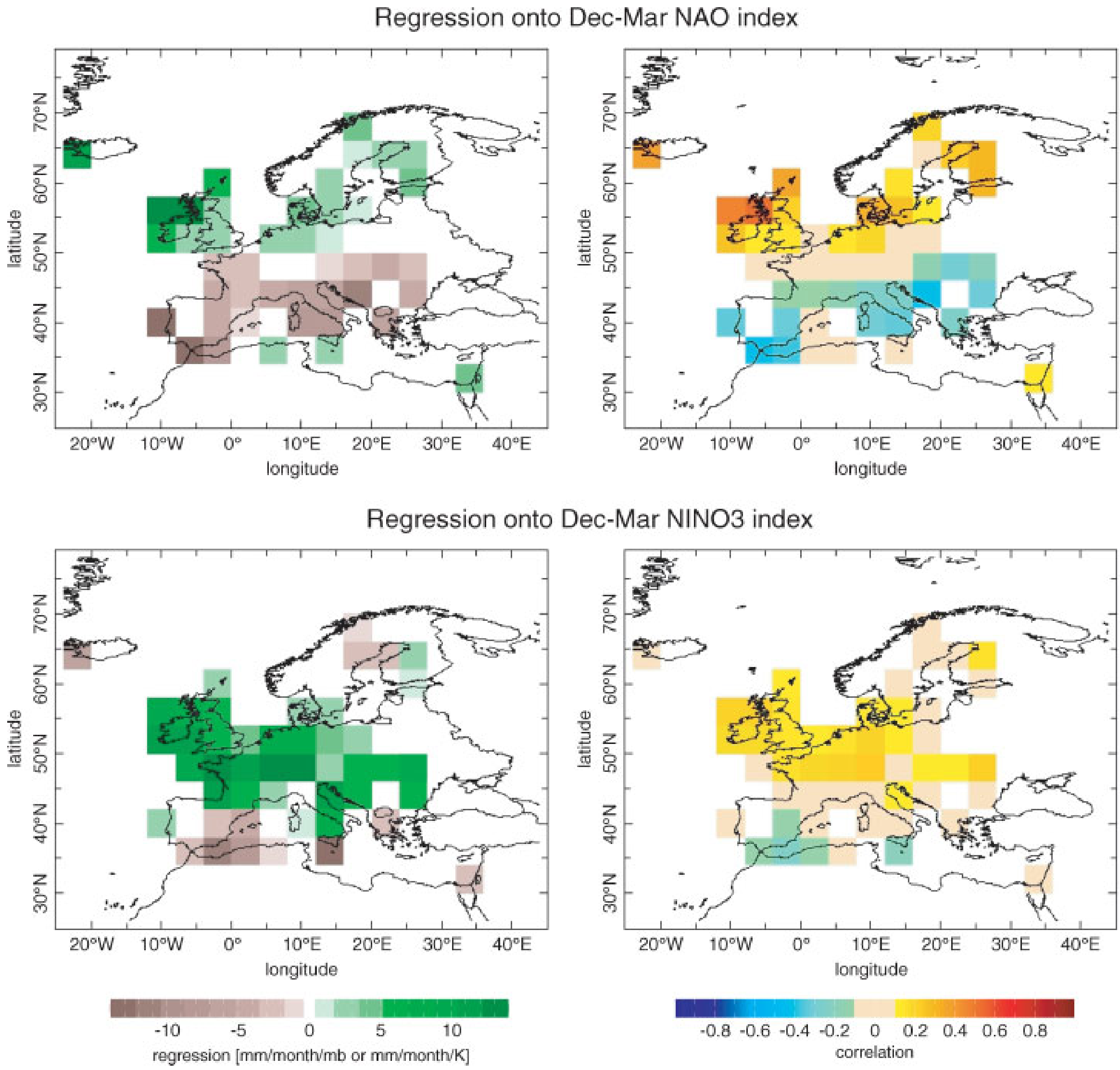

Figure 6. Multivariate regression of the observed GHCN 4° × 4° gridded station data precipitation anomaly on to the 6-year low-pass filtered: (a) NAO index (mm/month/mb); (c) NINO3 index (mm/month/K). Corresponding correlation coefficients are shown in (b) and (d). Correlation coefficients greater than or equal to 0.23 are significant at $p < 0.2$.

of the 1998–2003 period is reproduced by the models and was also likely forced from the tropics as suggested by Hoerling and Kumar (2003). The results add some support to the contention that, in addition to the NAO influence, and amidst considerable internal variability, there is a modest tropical Pacific SST influence on precipitation in this region (Mariotti *et al*., 2005).

The wetness of southern South America during the most recent mid-latitude drought regime is clearly very different to the global footprint of the five preceding major mid-latitude droughts since 1856. Liebmann *et al.* (2004) also note a recent positive trend in South American precipitation centred over southern Brazil, which they relate to a positive trend in SST in the nearby Atlantic Ocean, although not causally. The inability of the GOGA model to capture the observed southern South American wetness could potentially arise, as for the European sector, from the model's inability to faithfully capture annular mode variability. The southern annular mode (SAM) is often defined as the leading mode of 700 mb heights south of 20 °S and describes a basically zonal mean oscillation of mass between the mid-latitudes and the Polar ice cap together with associated changes in winds and temperature, and arises from interactions between transient eddies and the zonal mean flow (L'Heureux and Thompson, 2005, and references therein). As shown by L'Heureux and Thompson (2005), over the post-1979 period, the SAM during southern summer is highly correlated with the inverted index of SSTs in the eastern tropical Pacific Ocean i.e. La Niña conditions excite the positive phase of the SAM.

Figure 7(a) shows the Global Precipitation Climatology Project (GPCP) satellite and station data precipitation regressed on the SAM index, as defined above, using NCEP-NCAR Reanalyis data. This result confirms the link between SAM and ENSO in that the global pattern of precipitation associated with the SAM (Figure 7(a)) is essentially the same as that associated with La Niña

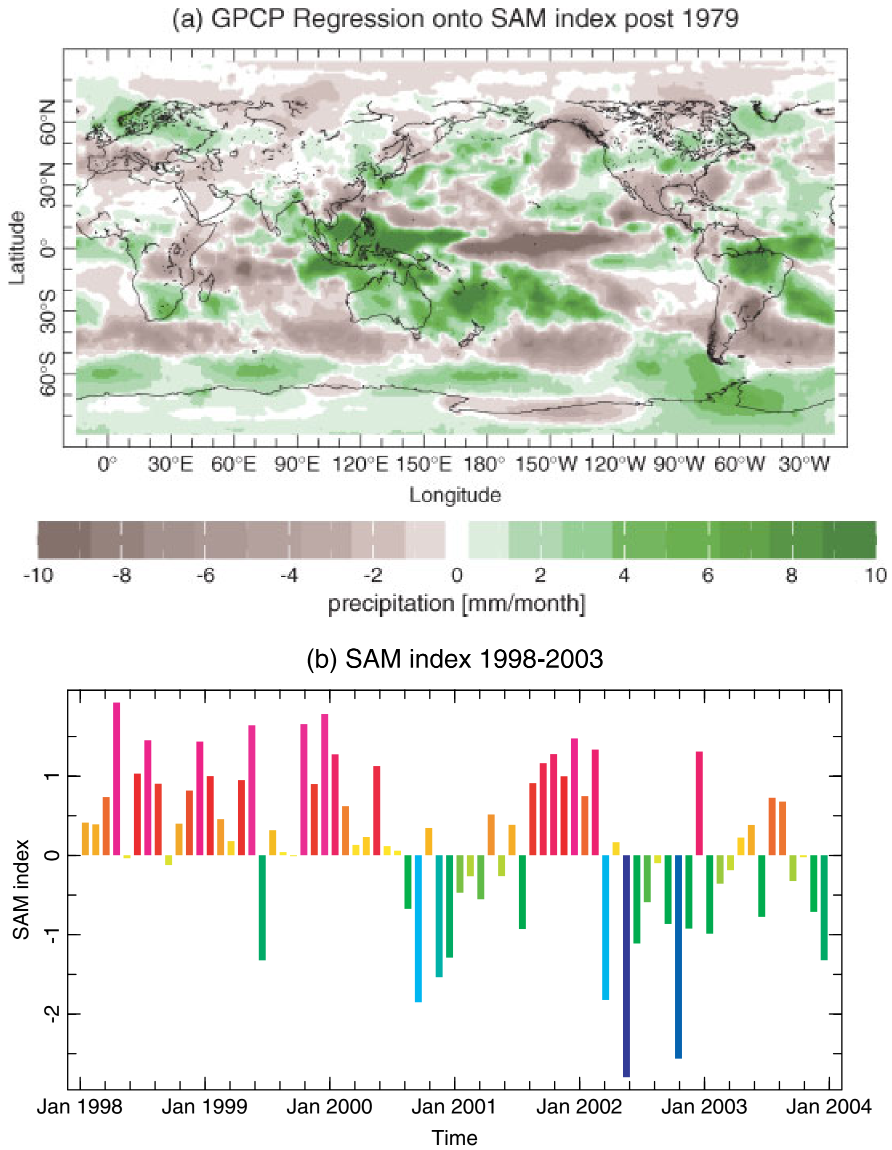

Figure 7. (a) The monthly mean GPCP v2 satellite-gauge precipitation anomaly regressed onto the SAM index from January 1979 to December 2004. (b) The SAM index from 1998 to 2003.

DOI: 10.1002/joc

(Figure 8(a), discussed in detail in Section 3). Like La Niña, the SAM tends to make southern South America dry. In the 1998–2003 period, the SAM was positive (Figure 7(b)), consistent with the coincident La Niña. Therefore the SAM provides no explanatory power beyond ENSO and the wetness in southern South America in recent years must have other causes. For the record, the POGA-ML and GOGA models both reliably produce the post-1979 behaviour of the SAM during southern summer (not shown), confirming dominance of ENSO-forcing of the SAM.

2.2.4. Summary

In summary, the spurious drought in Europe in the 1930s, and the recent wetness in southern South America aside, the GOGA and POGA-ML models do an impressive job at capturing the large-scale footprint of the persistent drought regimes of the last 150 years. Each of the six droughts is marked by the persistence of anomalously cool east central tropical Pacific SSTs, despite differences in the SSTAs of the Indian Ocean, Atlantic Ocean and north Pacific Ocean. The similarity of the POGA-ML and GOGA models cements the contention that the component of persistent extra-tropical drought/wetness that is SST forced, is forced from the tropical Pacific-a La Niña-like tropical Pacific.

3. The low-frequency ENSO/mid-latitude drought signal

By regressing the GHCN precipitation data onto the six-year low-pass filtered NINO 3 (NINO 3 is an index that

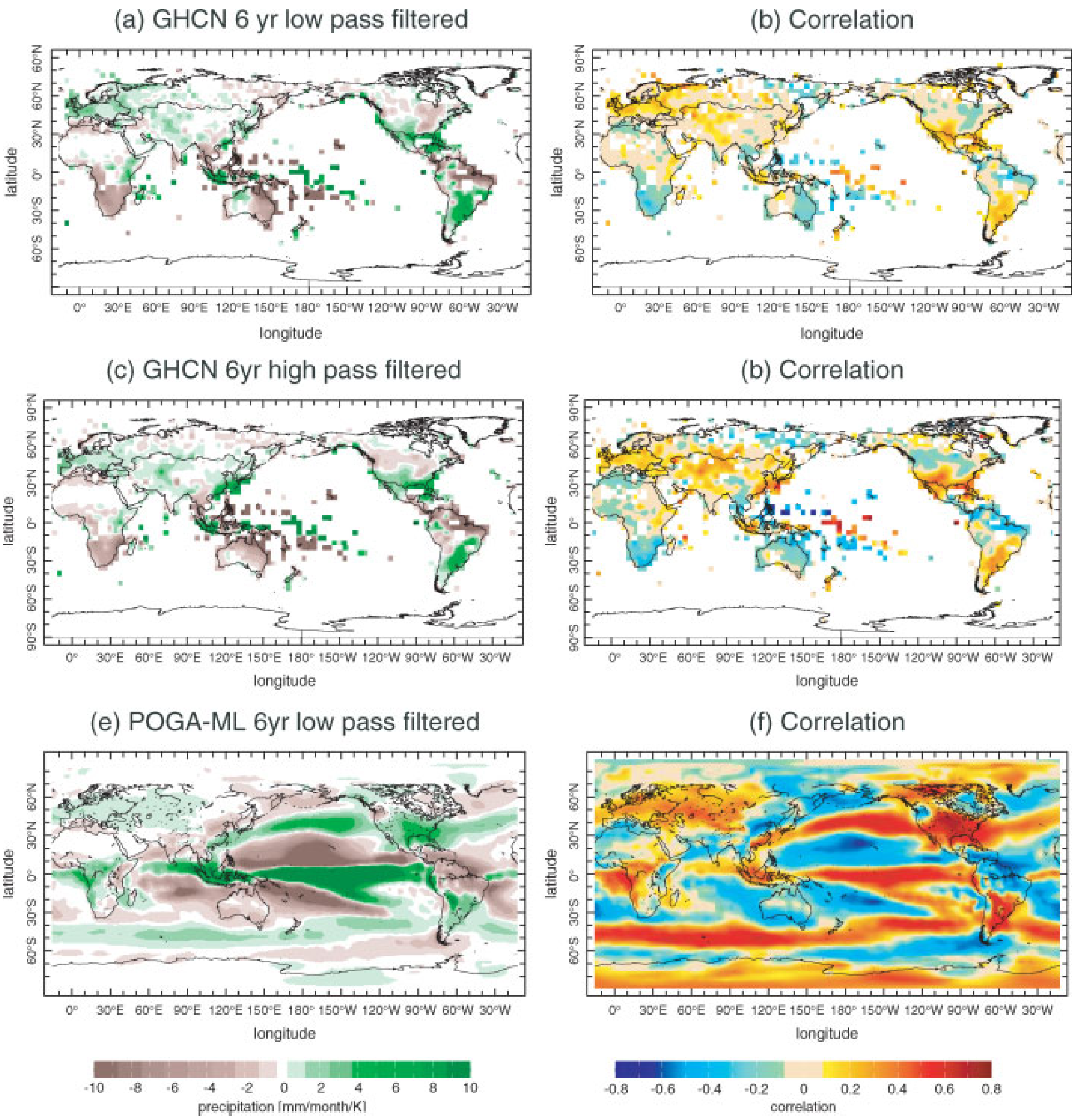

Figure 8. The Dec-May GHCN precipitation anomaly regressed on to the (a) 6-year low-pass, or (c) 6-year high-pass filtered Kaplan NINO 3 index. The corresponding correlation coefficients are shown in panels (b) and (d). The Dec-May POGA-ML precipitation anomaly regressed onto the low pass filtered Kaplan NINO 3 index (e) and the respective correlation coefficients (f). Each calculated over the period from 1857 to 2004.

DOI: 10.1002/joc

measures the strength of an ENSO event: it is the SST averaged over a region in the eastern equatorial Pacific (90°–150 °W, 5 °N–5 °S)) index (Kaplan *et al*., 2003) we can directly isolate the precipitation variability that arises as part of the low-frequency ENSO signal (Figure 8(a). This is done for the months of December through May (the months of greatest NINO3 variability) from 1857 to 2004. The corresponding correlation coefficients are shown in Figure 8(b). Analogous figures of the 6-year high-pass filtered case, representative of interannual ENSO variability, are also shown (Figure 8(c) and (d)). For the high-pass filtered case, a correlation coefficient of 0.16 is required for significance at the 95% level. Low-pass filtering of the data necessitates a higher degree of correlation for statistical significance. The pattern of low-frequency ENSO-related precipitation variability is strikingly similar to the interannual case. On interannual timescales, a cold eastern tropical Pacific corresponds to a dry southwestern United States, southern South America (Uruguay, north and central Argentina and southern Brazil), central and eastern Europe, central western Asia, equatorial eastern Africa (Kenya, Tanzania and Somalia), southern India and Sri Lanka, and wet areas in southern Africa, Mediterranean north Africa, eastern Australia, northeast South America and parts of the eastern United States. Due to the limited length of the observational record, only the extra-tropical drought regions in the southwestern United States, southern South America and (marginally) parts of central Europe and central western Asia have correlation coefficients that qualify as statistically significant at the 80% level.

Whilst these correlations are low, the model simulations add weight to the argument that the tropical Pacific-extra-tropical precipitation relationships on multi-year timescales are real: the POGA-ML model produces a pattern of precipitation variations noticeably similar to that observed, but with statistically significant correlations across North America, Europe, Asia as well as in the southern hemisphere mid-latitudes (Figure 8(f)). Lower correlations between tropical Pacific SSTs and precipitation observations are expected because the observations are an incomplete record of a single realization and hence include both sampling error and a sizable component due to internal atmospheric variability. In contrast, the model simulations near-perfectly isolate the SST-forced component and make clear that, amidst much precipitation variability generated by internal atmospheric variability, tropical Pacific SSTs do have a discernible impact on precipitation across the mid-latitudes.

On the basis of these arguments it seems fair to state that the large-scale relationships between regions of persistent extra-tropical drought/wetness outlined in Section 2, arise as part of a global response to low-frequency ENSO varibility. A La Niña-like tropical Pacific on decadal timescales, causes mid-latitude drought in North and South America, as well as drought in much of central Europe, central east Africa, southern India and Sri Lanka, and parts of western Australia. Noticeably, low-frequency precipitation variability in the northeast Brazil region (Figure 2) does not always fit into this pattern of global hemispheric and zonal symmetry (Figure 8). Precipitation in this region is strongly influenced by the meridional gradient of tropical Atlantic SST (e.g. Servain, 1991; Uvo *et al*., 1998), which is in part controlled by ENSO variability but also has a local Atlantic origin (Saravanan and Chang, 2000; Pezzi and Cavalcanti, 2001; Giannini *et al*., 2004). As both, ENSO and tropical Atlantic variability (TAV), add up to force precipitation anomalies in northeast Brazil, variability local to the tropical Atlantic can at times disrupt the hemispherically symmetric pattern.

4. Conclusions

Analysis of historical station precipitation data indicates that each major North American drought of the last 150 years appears as part of a larger, global pattern of low-frequency precipitation variability. There is a clear hemispherically and, in the extra-tropics, zonally symmetric component to this variability, such that when the tropical eastern Pacific and tropical troposphere are cooler than normal, much of the mid-latitudes are warm and dry. This feature is related to a low-frequency realization of the TMMEs mechanism described in detail by Seager *et al.* (2003, 2005a,b). Zonal asymmetries arise due to Rossby wave propagation from the cooler tropical Pacific, which regionally enhance or diminish the tendency for mid-latitude drought (Seager *et al*., 2005b). That this global pattern of multi-year extra-tropical drought regimes occurs in nature is demonstrated here for the first time. In particular, regions of enhanced and in-phase extra-tropical drought include western North America and southern South America, each under the downstream influence of Rossby wave propagation from a colder than normal tropical Pacific. Other regions of in-phase drought include western Australia, parts of Europe, and central east Africa, whilst other tropical land regions tend to be wet.

Model ensemble simulations forced by observed SSTs, globally (GOGA), and only from within the tropical Pacific (POGA-ML), were both able to capture the large-scale footprint of the global drought regimes since 1856, including the hemispheric symmetry and the zonal symmetry in the extra-tropics. The implication is that, as demonstrated for the western North American sector (Schubert *et al*., 2004b; Herweijer *et al*., 2005; Seager *et al*., 2005a), the major extra-tropical droughts of this period are primarily forced by tropical Pacific SSTs. In particular, sustained La Niña-like conditions correspond to persistent drought in southern South America (Uruguay, southern Brazil and north and central Argentina), and much of Europe, as observed. Contemporaneous drought in western Australia also occurs in the observations, but is not captured by the model simulations. In agreement with the instrumental record, rainfall anomalies of the opposite sign occur over most of the tropics (i.e. in particular over tropical central and South

DOI: 10.1002/joc

America, the Sahel) and over north Africa, and south Africa. Northeast Brazil, which is influenced by tropical Atlantic SSTs, and eastern Australia, both experience persistent precipitation anomalies but do not fit easily into this pattern, and neither model configurations reliably reproduce the precipitation histories in these regions.

During the most recent North American drought (shown here as 1998–2003), warming of all surface waters outside of the east central tropical Pacific appears to have interrupted this global pattern to some extent. In particular, the drought in North America is no longer mirrored in southern South America while the Sahel has remained dry. This aside, the global pattern of precipitation anomalies for the most recent drought is similar to that during the five prior droughts. The influence of the SAM is ruled out as an explanation for the wetness in southern South America. Rather, the precipitation response to the observed high polarity SAM index is shown to be similar to that of the cold phase of ENSO, both acting to make southern South America dry. A companion study to this one by Seager (2007), which focuses solely on the recent 'turn-of-the century drought', leaves us with a similar conclusion that midlatitude South America is wet during this recent period, for 'unexplained reasons'.

Our findings imply that atmospheric circulation changes associated with decadal ENSO-like climate variability are largely responsible for inducing the long-term interhemispheric extra-tropical drought and wetness regimes of the instrumental record. There is a strong spatial similarity to the hydroclimatic response to interannual ENSO-like climatic variability. On the heels of this study, several relevant studies by the authors have further investigated the global pattern of low-frequency drought variability. Seager (2007) examine the causes and global context of 'turn-of-the-century' drought, while Herweijer *et al*. (2007) look at the global hydroclimatic ÕfootprintÕ of the North American Medieval 'megadroughts'. In the latter study, the authors reveal a pattern of climate anomalies that largely matches the global hydroclimatic regime accompanying modern day North American drought. In-phase with the Medieval megadroughts of the American west, drought conditions occur in southern South America, central east Africa and much of Europe, while tropical land regions including the tropical Americas and the African Sahel are wet (Herweijer *et al*., 2007). In each case-present day and Medieval-a protracted La Niña-like tropical Pacific is associated with this pattern.

With regard to future hydroclimatic implications under greenhouse warming, a more La Niña-like tropical Pacific would create a tendency for persistent drought across the extra-tropical and tropical regions sensitive to tropical Pacific SST variability (in particular, western North America, southern South America, parts of Europe, western Australia and equatorial east Africa). A recent study by Seager *et al*. (2007) using the IPCC (Intergovernmental Panel for Climate Change) climate model projections of the twenty-first century shows widespread consensus that the American southwest and much of the subtropics, shifts rapidly to a climate of greater aridity. As the models vary in their tropical SST response to anthropogenic forcing, this is distinct from the historical droughts shown in the present study. The historical drought events are each attributed to changes in tropical SSTs, and while persistent La Niña events in the future will continue to cause drought, these will occur around a drier base state. In today's globalized economy, the reality of such concurrent and severe drought in several agriculturally productive regions of the world could undoubtedly have a profound social and economic impact.

Acknowledgements

Many thanks to Naomi Naik for performing the model simulations and to Ed Cook, Yochanan Kushnir and Mark Cane for many discussions. CH was supported by a NASA Grant NNG04GQ55H. RS was supported by NOAA Grants NAO30AR4320179 P07 and 20A and NSF grants ATM 05-01878 and ATM 0347009. The model data for the GOGA and POGA-ML simulations can be downloaded or analysed and visualized online:

http://kage.ldeo.columbia.edu:81/SOURCES/.LDEO/.ClimateGroup/.PROJECTS/.CCM3/.

References

Allan RJ, Dárrigo RD. 1999. "Persistent" ENSO sequences: How unusual was the 1990–1995 El Niño? *Holocene* **9**: 101–118.

Barsugli JJ, Battisti DS. 1998. The basic effects of atmosphereocean thermal coupling on midlatitude variability. *Journal of the Atmospheric Sciences* **55**: 477–493.

Bretherton CS, Battisti DS. 2000. An interpretation of the results from atmospheric general circulation models forced by the time history of the observed sea surface temperature distribution. *Geophysical Research Letters* **27**(6): 767–770.

Briffa KR, Jones PD, Hulme M. 1994. Summer moisture variability across Europe, 1892–1991: an analysis based on the Palmer Drought Severity Index. *International Journal of Climatology* **14**: 475–506.

Casty C, Luterbacher J, Wanner H, Esper J, Boehm R. 2005. Temperature and precipitation variability in the European Alps since 1500. *International Journal of Climatology* **25**: 1855–1880.

Cole J, Overpeck JT, Cook ER. 2002. Multi-year La Nina events and persistent drought in the contiguous United States. *Geophysical Research Letters* **29**: 1647–1650.

Compagnucci RH, Agosta EH, Vargas WM. 2002. Climate change and quasi-oscillations in central-west Argentina summer precipitation: main features and coherent behaviour with southern African region. *Climate Dynamics* **18**: 421–435.

Dai A, Fung IY, Del Genio AD. 1997. Surface observed global land precipitation variations during 1900–1988. *Journal of Climate* **10**: 2943–2962.

Eischeid JK, Diaz HF, Bradley RS, Jones PD. 1991. *A Comprehensive Precipitation Data Set for Global Land Areas*, DOE/ER-6901T-H1. Carbon Dioxide Research Division, U.S. Department of Energy: Washington, DC.

Endfield GH, Nash DJ. 2002. Drought, desiccation and discourse: missionary correspondence and nineteenth century climate change in central southern Africa. *Geographical Journal* **161**(1): 33–47.

Evans T. 1990. History of Nile flows. In *The Nile*, Howell PP, Allen JA (eds). School of Oriental and African Studies, University of London: London; 5–40.

Fye FK, Stahle DW, Cook ER. 2003. Paleoclimate analogs to Twentieth Century moisture regimes across the United States. *Bulletin of the American Meteorological Society* **84**: 901–909.

Fye FK, Stahle DW, Cook ER. 2004. Twentieth-Century sea surface temperature patterns in the Pacific during decadal moisture regimes over the United States. *Earth Interactions* **8**: 1–22.

Giannini A, Saravanan R, Chang P. 2003. Oceanic forcing of Sahel rainfall on interannual to interdecadal time scales. *Science* **302**: 1027–1030.

Giannini A, Saravanan R, Chang P. 2004. The preconditioning of tropical Atlantic variability in the development of the ENSO teleconnection: Implications for the prediction of Nordeste rainfall. *Climate Dynamics* **22**: 839–855.

Goddard L, Graham NE. 1999. Importance of the Indian Ocean for simulating rainfall anomalies over eastern and southern Africa. *Journal of Geophysical Research* **104**: 19099–19116.

Hastenrath S, Heller L. 1977. Dynamics of climate hazards in northeast Brazil. *Quarterly Journal of the Royal Meteorological Society* **103**: 77–92.

Herweijer C, Seager R, Cook ER. 2006. North American Droughts of the mid-to-late Nineteenth Century: a history, simulation and implication for Medieval drought. *Holocene* **16**: 159–171.

Herweijer C, Seager R, Cook ER, Emile-Geay J. 2007. North American Droughts of the last Millennium from a Gridded Network of Tree-ring Data. *Journal of Climate* **20**: 1353–1376.

Hoerling MP, Kumar A. 2003. The perfect ocean for drought. *Science* **299**: 691–699.

Hoerling MP, Hurrell JW, Xu T. 2001. Tropical origins for recent North Atlantic climate change. *Science* **292**: 90–92.

Huang H-P, Seager R, Kushnir Y. 2005. The 1976/77 transition in precipitation over the Americas and the influence of tropical sea surface temperature. *Climate Dynamics* **24**: 721–740.

Hulme M, Jones PD. 1994. Global climate change in the instrumental period. *Environmental Pollution* **83**: 23–36.

Hurrell JW. 1995. Decadal trends in the North Atlantic Oscillation region temperatures and precipitation. *Science* **269**: 676–679.

Hurrell JW. 1996. Influence of variations in extratropical wintertime teleconnections on Northern Hemisphere temperature. *Geophysical Research Letters* **23**: 665–668.

Hurrell JW, Kushnir Y, Visbeck M, Ottersen G. 2003. In *An Overview of the North Atlantic Oscillation. The North Atlantic Oscillation: Climate Significance and Environmental Impact*, *Geophysical Monograph Series, 134*, American Geophys Union; 1–35.

Kaplan A, Cane MA, Kushnir Y. 2003. Reduced space approach to the optimal analysis interpolation of historical marine observations: accomplishments, difficulties, and prospects. In *Advances in the Applicationsof Marine Climatology: The Dynamic Part of the WMO Guide to the Applications of Marine Climatology*, WMO/TD-1081. World Meteorological Organization: Geneva; 199–216.

Kaplan A, Cane MA, Kushnir Y, Clement AC, Blumenthal MB, Rajagopalan B. 1998. Analyses of global sea surface temperature: 1856–1991. *Journal of Geophysical Research* **103**: 18567–18589.

Kiehl JT, Hack JJ, Bonan GB, Bovile BA, Williamson DL, Rasch PJ. 1998. The national center for atmospheric research community climate model: CCM3. *Journal of Climate* **11**: 1131–1149.

Kushnir Y, Robinson WA, Blade I, Hall NMJ, Peng S, Sutton RT. 2002. Atmospheric GCM response to extratropical SST anomalies: synthesis and evaluation. *Journal of Climate* **15**: 2233–2256.

L'Heureux ML, Thompson DWJ. 2005. Observed relationships between the El Nino/Southern Oscillation and the extratropical zonal-mean circulation. *Journal of Climate* **19**: 276–277.

Liebmann B, Vera CS, Carvalho LMV, Camilloni IA, Hoerling MP, Allured D, Barros VR, Báez J, Bidegain M. 2004. An observed trend in central South American precipitation. *Journal of Climate* **17**: 4357–4367.

Lindesay JA, Vogel CH. 1990. Historical evidence for Southern Oscillation-southern African rainfall relationships. *International Journal of Climatology* **10**: 679–689.

Mariotti A, Ballabrera-Poy J, Zeng N. 2005. Tropical influence on Euro-Asian autumn rainfall variability. *Climate Dynamics* **24**: 511–521.

Mechoso CR, Iribarren GP. 1992. Streamflow in Southeastern South America and the Southern Oscillation. *J Climate* **5**: 1535–1539.

Merkel U, Latif M. 2002. A high-resolution AGCM study of the El Nino impact on the North Atlantic/European sector. *Geophysical Research Letters* **29**: 1291–1294.

Meshcherskaya AV, Blazhevich VG. 1997. The drought and excessive moisture indices in a historical perspective in the principal grain-producing regions of the Former Soviet Union. *Journal of Climate* **10**: 2670–2682.

Moura AD, Shukla J. 1981. On the dynamics of drought in northeast Brazil: observations, theory and numerical experiments with a general circulation model. *Journal of the Atmospheric Sciences* **38**: 2653–2675.

Nash DJ, Endfield GH. 2002. A 19th Century climate chronology for the Kalahari region of central southern Africa derived from Missionary correspondance. *International Journal of Climatology* **22**: 821–841.

Nicholson SE. 1998. Fluctuations of rift valley lakes malawi and chilwa during historical times: a synthesis of geological, archaeological and historical information. In *Environmental Change and Response in East African Lakes*, Lehman JT (ed.). Kluwer Academic Publishers: Dordrecht; 207–231.

Nicholson SE. 1999. Historical and modern fluctuations of lakes tanganyika and rukwa and their relationship to rainfall variability. *Climatic Change* **41**: 43–71.

Nicholson SE. 2001. Climatic and environmental change in Africa during the last two centuries. *Climate Research* **17**: 123–144.

Nicholson SE, Yin X. 2001. Rainfall conditions in equatorial East Africa during the nineteenth century as inferred from the record of lake victoria. *Climatic Change* **48**: 387–398.

Owen RB, Crossley R. 1989. Recent sedimentation in lakes Chilwa and Chiuta, Malawi. *Palaeoecology of Africa* **20**: 109–117.

Pezzi LP, Cavalcanti IFA. 2001. The relative importance of ENSO and tropical Atlantic sea surface temperature anomalies for seasonal precipitation over South America: a numerical study. *Climate Dynamics* **15**: 205–212.

Preito MR, Herrera R, Dussel P. 1999. Historical evidences of streamflow fluctuations in the Mendoza river, Argentina, and their relationships with ENSO. *Holocene* **9**: 473–481.

Quinn WH. 1993. The large-scale ENSO event, the El Ni no and other important regional features. *Bulletin d'Institut Francais d'Etudes Andines* **22**: 13–34.

Quinn WH, Neal VT. 1992. The historical record of El Niño events. In *Climate Since 1500*, Bradley RS, Jones PD (eds). Routledge, Chapman and Hall: London; 623–648.

Rayner N, Parker D, Horton E, Folland C, Alexander L, Rowell D, Kent E, Kaplan A. 2003. Global analyses of sea surface temperature, sea ice, and night marine air temperature since the late nineteenth century. *Journal of Geophysical Research* **108**: 4407–4437. 10.1029/2002JD002670.

Riehl H, El-Bakry M, Meitin J. 1979. Nile river discharge. *Monthly Weather Review* **107**: 1546–1553.

Robertson AW, Mechoso CR. 1998. Interannual and decadal cycles in river flows in Southeastern South America. *Journal of Climate* **11**: 2570–2581.

Robinson WA. 2000. Review of WETS – the workshop on extra-tropical SST anomalies. *Bulletin of the American Meteorological Society* **81**(3): 567–577.

Robinson WA. 2005. Eddy-mediated interactions between low latitudes and the extratropics. In *The Global Circulation of the Atmosphere*, Schneider T, Sobel A (eds). Princeton University Press: Princton, NJ.

Rodwell MJ, Rodwell DP, Folland KC. 1999. Oceanic Forcing of the wintertime North Atlantic Oscillation and European Climate. *Nature* **398**: 320–323.

Saravanan R, Chang P. 2000. Interaction between tropical Atlantic variability and El Nino-Southern Oscillation. *Journal of Climate* **13**: 2177–2194.

Schoengart J, Junk WJ, Piedade MTF, Ayres JM, Huttermann A, Worbes M. 2004. Teleconnection between tree growth in the Amazonian floodplains and the Ni no-Southern Oscillation effect. *Global Change Biology* **10**: 683–692.

Schubert SD, Suarez MJ, Region PJ, Koster RD, Bacmeister JT. 2004a. Causes of long-term drought in the United States Great Plains. *Journal of Climate* **17**: 485–503.

Schubert SD, Suarez MJ, Pegion PJ, Randal RD, Bacmeister JT. 2004b. On the cause of the 1930s Dust Bowl. *Science* **303**: 1855–1859.

Scian B, Donnari M. 1997. Retrospective analysis of the Palmer Drought Severity Index in the semi-arid Pampas region, Argentina. *International Journal of Climatology* **17**: 313–322.

Seager R. 2007. The Turn of the Century drought across North America: global context, dynamics and past analogues. *Journal of Climate* **20**: 5527–5552.

Seager R, Harnik N, Kushnir Y, Robinson W, Miller J. 2003. Mechanisms of hemispherically symmetric climate variability. *Journal of Climate* **16**: 2960–2978.

Seager R, Kushnir Y, Herweijer C, Naik N, Miller J. 2005a. Modeling of tropical forcing of persistent droughts and pluvials over western North America: 1856–2000. *Journal of Climate* **18**: 4068–4091.

Seager R, Harnik N, Robinson WA, Kushnir Y, Ting M, Huang JVHP. 2005b. Mechanisms of ENSO-forcing of hemispherically symmetric precipitation variability. *Quarterly Journal of the Royal Meteorological Society* **131**: 1501–1527.

Seager R, Kushnir Y, Visbeck MH, Naik N, Miller J, Krahmann G, Cullen HM. 2000. Causes of Atlantic Ocean climate variability between 1958 and 1998. *Journal of Climate* **13**: 2845–2862.

Seager R, Ting MF, Held IM, Kushnir Y, Lu J, Vecchi G, Huang H-P, Harnik N, Leetmaa A, Lau N-C, Li C, Velez J, Naik N. 2007. Model projections of an imminent transition to a more arid climate in Southwestern North America. *Science* **316**: 1181–1184.

Servain J. 1991. Simple climatic indices for the tropical Atlantic ocean and some applications. *Journal of Geophysical Research* **96**: 15137–15146.

Shindell DT, Miller RL, Schmidt G, Pandolfo L. 1999. Simulation of recent northern winter climate trends by greenhouse-gas forcing. *Nature* **399**: 452–455.

Sieger R. 1887. *Schwankungen der Innerafrikanischen Seen*, Bericht, XIII, Vereinsjahr. Vereine der Geographen an der Universitaet Wien, Vienna; Austria; 41–60.

Sieger R. 1888. *Neue Beitraege zur Statistik der Seespiegelschwankungen*. Bericht, XIV, Vereinsjahr. Vereine der Geographen an der Universitaet Wien, Vienna; Austria; 11–24.

Sutton RT, Hodson DLR. 2005. Atlantic ocean forcing of North American and European summer climate. *Science* **309**: 115–118.

Touchan R, Xoplaki E, Funkhouser G, Luterbacher J, Hughes MK, Erkan N, Akkemik U, Stephan J. 2005. Reconstructions of spring/summer precipitation for the Eastern Mediterranean from tree-ring widths and its connection to large-scale atmospheric circulation. *Climate Dynamics* **25**: 75–98.

Trenberth K, Branstator GW. 1992. Issues in establishing causes of the 1988 drought over North America. *Journal of Climate* **5**: 159–172.

Trenberth K, Guillemot CJ. 1996. Physical processes involved in the 1988 drought and 1993 floods in North America. *Journal of Climate* **9**: 1288–1298.

Uvo CB, Repelli CA, Zebiak SE, Kushnir Y. 1998. The relationships between tropical Pacific and Atlantic SST and Northeast Brazil monthly precipitation. *Journal of Climate* **11**: 551–561.

Verschuren D. 2001. Reconstructing fluctuations of a shallow East African lake during the past 1800 yrs from sediment stratigraphy in a submerged crater basin. *Journal of Paleolimnology* **25**: 297–311.

Villalba R, Grau HR, Boninsegna JA, Jacoby GC, Ripalta A. 1998. Tree-ring evidence for longterm precipitation changes in subtropical South America. *International Journal of Climatology* **18**: 1463–1478.

Visbeck MH, Chassignet E, Curry R, Delworth T, Dickson B, Krahmann G. 2003. The Ocean's response to North Atlantic Oscillation variability. In *The North Atlantic Oscillation*, *Geophysical Monograph Series, 134*, Hurrell JW, Kushnir Y, Ottersen G, Visbeck M (eds), American Geophys Union; 113–146.

Walsh RPD, Musa HRJ. 1994. Flood frequency and impacts at Khartoum since the early nineteenth century. *Geographical Journal* **160**: 266–274.

Woodhouse CA, Overpeck JT. 1998. 2000 years of drought variability in the central United States. *Bulletin of the American Meteorological Society* **79**: 2693–2714.